ELSEVIER

Journal of Power Sources 111 (2002) 329–334

JOURNAL OF POWER SOURCES

www.elsevier.com/locate/jpowsour

Modified natural graphite as anode material for lithium ion batteries

Y.P. Wu[a,b,*], C. Jiang[a], C. Wan[a], R. Holze[b]

[a]*Division of Chemical Engineering, INET, Tsinghua University, Beijing 102201, PR China*
[b]*Technische Universität Chemnitz, Institut für Chemie, AG Elektrochemie, D-09107 Chemnitz, Germany*

Received 8 December 2001; received in revised form 27 May 2002; accepted 3 June 2002

Abstract

A concentrated nitric acid solution was used as an oxidant to modify the electrochemical performance of natural graphite as anode material for lithium ion batteries. Results of X-ray photoelectron spectroscopy, electron paramagnetic resonance, thermogravimmetry, differential thermal analysis, high resolution electron microscopy, and measurement of the reversible capacity suggest that the surface structure of natural graphite was changed, a fresh dense layer of oxides was formed. Some structural imperfections were removed, and the stability of the graphite structure increased. These changes impede decomposition of electrolyte solvent molecules, co-intercalation of solvated lithium ions and movement of graphene planes along the *a*-axis direction. Concomitantly, more micropores were introduced, and thus, lithium intercalation and deintercalation were favored and more sites were provided for lithium storage. Consequently, the reversible capacity and the cycling behavior of the modified natural graphite were much improved by the oxidation. Obviously, the liquid–solid oxidation is advantageous in controlling the uniformity of the products.

Keywords: Lithium ion batteries; Natural graphite; Nitric acid; Anode material

1. Introduction

Lithium ion batteries have many advantages as compared to traditional rechargeable batteries, and their development is very rapid since their birth at the end of 1980s and in the early 1990s. Though many kinds of anode materials have been investigated, graphitic carbon is still the main candidate. Consequently, modification of graphite became a recent focus. For example, graphite is mildly oxidized by air, oxygen, carbon dioxide, and ozone, or fluorinated by fluorine gas [1–7]. Other kinds of carbonaceous materials can also be coated onto the surface of graphite such as pitch coke, phenol-formaldehyde resin and pyrolytic carbon from chemical vapor deposition [1,8–16]. Metals and metal oxides can be deposited onto the surface of natural graphite such as silver, copper and its oxides, aluminum, and nickel [17–22], and the obtained composites as anode materials show considerably improved electrochemical performance. After coating polymers such as gelatin and epoxy resin by dipping in their solutions, irreversible capacity in the first cycle decreased [23,24]. All these kinds of improvements were due to cover-up/removal of some active sites at the surface of graphite. Of course, other kinds of effects were also in action at the same time such as alloying of lithium with the deposited metals. The complexity of research and development is further increased by the variety of available graphitic carbons, and differences in source, treatment, and processing resulting in striking differences in the surface and the volume structure.

Recently, we have investigated one kind of natural graphite from China [4], and its reversible capacity was low, about 250 mAh g^{-1}, and capacity faded to 100 mAh g^{-1} within 10 cycles. This performance is much inferior to data reviewed above. When catalysts for oxidation were deposited onto its surface, its electrochemical performance improved much after the chemical and the catalytic oxidation, and the reversible capacity could be >372 mAh g^{-1}, viz. the theoretical value of graphite [4]. However, in gas–solid interphase oxidation reaction control of the homogeneity of the products is difficult to maintain. Consequently, a liquid–solid interface oxidation reaction has been introduced such as the use of chemical oxidants $(NH_4)_2S_2O_8$, H_2O_2, $Ce(SO_4)_2$ [25–27], and their standard potentials (E_0) are 2.08, 1.78 and 1.61 V for $S_2O_8^{2-}/SO_4^{2-}$, H_2O_2/H_2O and Ce^{4+}/Ce^{3+}, respectively.

* Corresponding author. Tel.: +49-371-531-1366x1477; fax: +49-371-531-1371.
E-mail addresses: wuyp99@hotmail.com (Y.P. Wu), rudolf.holze@chemie.tu-chemnitz.de (R. Holze).

0378-7753/02/$ – see front matter
PII: S0378-7753(02)00349-X

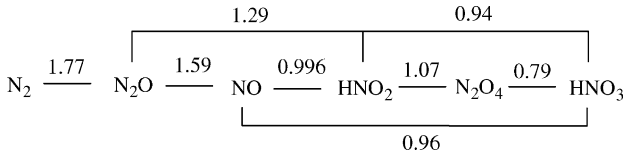

Fig. 1. The standard potentials for nitrogen compounds in acidic solution (E_0/V).

Nitric acid is well known as a strong oxidant. As indicated in Fig. 1, the standard potentials of its partial decomposition products can be >1.5 V. When its solution is heated, its oxidation capability will increase further. Consequently, here we used nitric acid solution as an oxidant to modify our common natural graphite, and initial results showed that this method was also satisfactory, and the actions of this oxidant were investigated.

2. Experimental

A natural graphite from China (designated as D) with interlayer distance d_{002} 3.351 Å and crystal size L_c 120 Å was dipped into concentrated nitric acid solution under stirring at $T = 20$, 60 and 100 °C, separately, for some time, and subsequently washed with water until neutral and dried. The prepared products were marked N1, N2 and N3, respectively.

X-ray photoelectron spectra (XPS) were obtained with an ES-300 spectrometer, and the relative contents of O and C at the surface of the natural graphite were calculated on the basis of their photoionization cross-sections and the integrals of their X-ray photoelectron intensities. Electron paramagnetic resonance (EPR) was measured with an EPR-200 spectrometer (Bruker, Germany). Thermogravimmetry and differential thermal analysis (TG-DTA) were performed with a PCT-1 under air, the heating rate was 20 °C min^{-1}. High resolution electron micrographs (HREM) were obtained with a EM-200CX microscope; samples were uniformly pre-dispersed on micro-nets with cavities of μm-size.

Capacity and cycling behavior were tested according to our reported method described elsewhere [4], which used lithium foil as the counter and reference electrode, 1 mol l^{-1} $LiClO_4$ solution in the mixture of EC/DEC (vol:vol = 3:7) as the electrolyte and homemade porous PP film as the separator. The anode was prepared by pressing the mixture of natural graphite and 5% wt.% binder PVDF dissolved in *N*,*N*′-dimethyl formamide into pellets with a diameter of ca. 1 cm. After drying under vacuum at 120 °C over night, the anode pellets were put into an argon box and assembled into model cells. Electrochemical performance was measured galvanostatically at 0.2 mA with a CT2001A cell test instrument (Wuhan LAND Electronic Co., Ltd., China), discharge (intercalation process) and charge (deintercalation process) voltages were ranged from 0.0 to 2.0 V versus Li^+/Li.

3. Results and discussions

There are a lot of structural imperfections and defects such as sp^3-hybridized carbon atoms, edge atoms and carbon chains in graphite [28–30] especially in natural graphite because of its incomplete graphitization during the natural formation process. These structures are prone to attack of oxidants and some of them would be removed after the oxidation reaction with the nitric acid solution. Consequently, the surface structure of the natural graphite D will be changed after the oxidation reaction.

XPS spectra of O 1s in the samples D and N2 are shown in Fig. 2 and selected data are summarized in Table 1. Four kinds of oxygen atom species are present, i.e. hydroxyl/phenolic group, ether oxygen, carboxylic oxygen in –COOR (R = H and alkyl) and carbonyl oxygen in acetone/quinone corresponding to binding energy peaks at 534.1, 533.2, 532.3 and 530.9 eV, respectively [25,31].

XPS spectra of C 1s in the samples D and N2 are shown in Fig. 3, and four kinds of carbon atoms species can be discerned, i.e. carbonyl carbon in acetone/quinone, carboxylic carbon in –COOR (R = H and alkyl), ether/phenolic carbon in C–O–C and C–OH, and carbon atoms in graphene planes corresponding to binding energy peaks at 288.9, 287.2, 285.9 and 284.4 eV, respectively [25,31].

Before the oxidation treatment natural graphite may chemi- and physisorb oxides like, e.g. water or CO_2 and oxygen. Moreover, the natural graphite used here was dipped in KOH solution to remove mineralic constituents. Consequently, four kinds of oxides were also observed like in the sample N2 after the oxidation treatment. In the present case, the relative content of carbonyl oxygen in acetone/quinone and those of carbonyl carbon in acetone/quinone, carbonyl

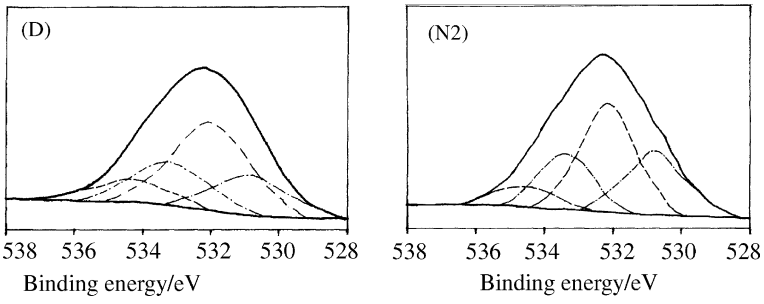

Fig. 2. XPS spectra of O 1s at the surface of natural graphite before (D) and after (N2) the oxidation treatment.

Table 1
Selected results obtained with natural graphite before (D) and after (N2) mild oxidation by nitric acid solution

Sample	Treatment temperature (°C)	Weight loss (%)	Atomic ratio of O at the surface (%)	Atomic ratio of C at the surface(%)	Species and contents of oxygen atoms				Species and contents of carbon atoms			
					534.1 eV	533.2 eV	532.3 eV	530.9 eV	288.9 eV	287.2 eV	285.9 eV	284.4 eV
D	–	–	4.11	95.89	0.1268	0.2320	0.4526	0.1886	0.0299	0.0534	0.1029	0.8138
N2	60	1.98	3.96	96.04	0.1006	0.2128	0.4188	0.2622	0.0438	0.0610	0.0902	0.8050

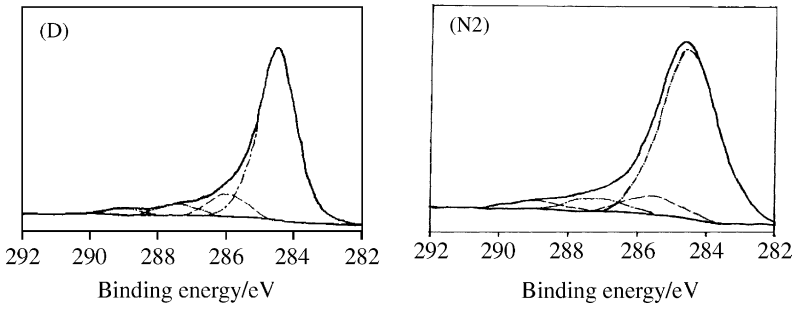

Fig. 3. XPS spectra of C 1s at the surface of natural graphite before (D) and after (N2) the oxidation treatment.

carbon in –COOR (R = H and alkyl) increased after the oxidation treatment as seen from the changes in the relative contributions of the peaks at 530.9, 288.9 and 287.2 eV. However, in contrast with results obtained with oxidative treatment with $(NH_4)_2S_2O_8$, H_2O_2 and $Ce(SO_4)_2$ [25,27], we could not obtain clear evidence indicating which kind(s) of compound(s) was(were) mainly changed. One reason is the presumably complicated oxidation reaction. Certainly weakly adsorbed oxygen atoms were removed and replaced by a layer of oxides from the oxidation bonded more firmly with the carbon structure [32] because there is a slight weight loss after the mild oxidation treatment (2.10, 1.98 and 1.76% for N1, N2 and N3, respectively). However, the change of the content of oxygen atoms at the surface as shown in Table 1 is different from those observed using $(NH_4)_2S_2O_8$, H_2O_2 and $Ce(SO_4)_2$ as chemical oxidants [25,27]. It decreased from 4.11 to 3.96%. Perhaps the reduction products of nitric acid were gaseous like, e.g. NO_2 and NO that might have reacted less effectively with the graphite. Therefore, instead of the assumed increase the content of oxygen at the surface of graphite decreased. In previously reported experiments [25], we tried to reoxidize an oxidized natural graphite. We found that the weight loss was much less than that from the first treatment. This clearly indicated that the active structural imperfections such as sp^3-hybridized carbon atoms, edge carbon atoms and carbon chains existed in the natural graphite and some of them were removed during the above oxidation treatment though their amounts were small and no method has been found to determine them precisely. Nitric acid acted in the same way since it is also a good oxidant.

EPR spectra of samples D and N2 are shown in Fig. 4. They indicate, that the relative concentration of free spins increased only slightly, from $9.79 \times 10^{11}\ g^{-1}$ (D) to $1.02 \times 10^{12}\ g^{-1}$ (N2). Though the *g*-factors for the free spins are practically the same, 2.0078 and 2.0079, the shapes of the signal are different. After the oxidation the signal became narrower. In natural graphite, there are several radical species before the oxidation, and their sum appears just like a single very broad signal. During the oxidation these radicals may react with HNO_3, and new radicals can be formed. Simultaneously, the mild oxidation eliminated some reactive structural imperfections such as carbon chains and sp^3-hybridized carbon atoms. During this process additional radicals may be formed. Most of these radicals are situated inside the graphite [25,27]. Since they were produced under the same condition, i.e. by the oxidation of HNO_3, the environment for the radicals is practically the same for all of them, thus, the inhomogenities causing the large line-width were diminished and the EPR spectrum showed a sharper line. In comparison with the oxidation treatment

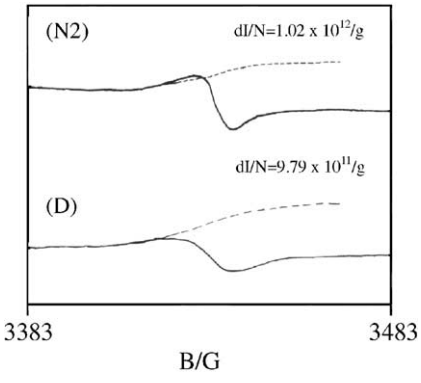

Fig. 4. EPR spectra of natural graphite before (D) and after (N2) the oxidation treatment measured at room temperature.

with $(NH_4)_2S_2O_8$ solution at 60 °C (2.87×10^{12} g^{-1}) and air at 550 °C (1.67×10^{12} g^{-1}) [27,33], the increase in the number of radicals was smaller. One reason is the lower oxidation ability of nitric acid as compared to that of $(NH_4)_2S_2O_8$. Another conceivable reason is low affinity of radicalic reduction products of HNO_3 towards binding on the graphite surface since nitric oxides can escape quickly as gases. As a result, radicals from nitric oxides will not spread extensively into the graphite structure. Of course, as shown in Fig. 1, some nitric oxides would act as oxidants to remove some imperfections. In the case of $(NH_4)_2S_2O_8$, it decomposes via a $\cdot HSO_4^{2-}$ radical ion, which can intercalate into the graphene planes, and thus, more radicals have been produced in graphite due to oxidative removal of imperfections [27].

These results are evidently different from those obtained with air as an oxidant for an NG-7 graphite [5]. In the latter case, it was found that the intensity of electron spin resonance or the number of radicals decreased sharply. This apparent contradiction is indicative of the rather complex EPR-behavior of carbon and graphite, which we cannot currently explain.

After removal of structural imperfections, the structure of the treated natural graphite became more stable. Curves of thermogravimmetric and differential thermal analysis (TG-DTA) of D and N2 are shown in Fig. 5. At first, the weight decreased slowly because of the thermal decomposition of less stable oxides and the slight oxidation. Subsequently, at temperatures beyond 500 °C combustion began and the curves of DTA increased. When the combustion occurred most rapidly, DTA curves peaked. After the oxidation treatment, the exothermal peaks shifted from 742 to 752 °C. This certainly supports the suggested changes although the exothermal peak shifted just slightly to a higher temperature. In comparison with samples treated with

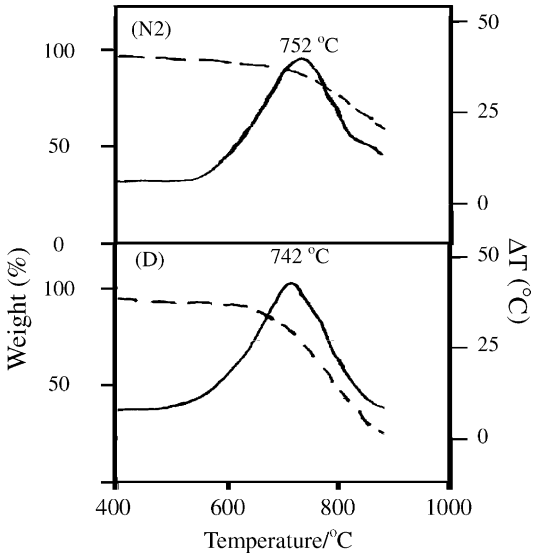

Fig. 5. Diagrams of TG-DTA of natural graphite before (D) and after (N2) the oxidation treatment ((- - -) TG curves; (—) DTA curves).

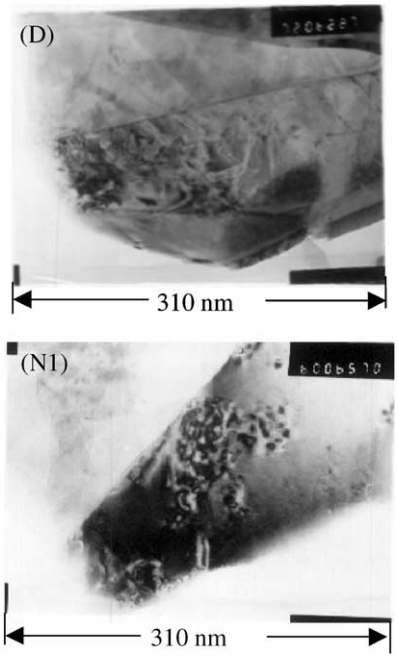

Fig. 6. HREM micrographs of natural graphite before (D) and after (N1) the oxidation treatment.

$(NH_4)_2S_2O_8$, this shift is smaller. In the latter case, the temperature of the exothermal peak increased to 761 °C. This once more suggests that the oxidation ability of HNO_3 is weaker than that of $(NH_4)_2S_2O_8$.

HREM micrographs of natural graphite D and N1 are shown in Fig. 6. They show a slight increase in the number of micropores and nanochannels after the oxidation. In our former experiment [27], the increase was much more pronounced and was also reflected in the inner specific surface area.

Discharge and charge profiles in the first cycle and discharge profiles in the second cycle of natural graphite D and the prepared sample N2 are presented in Fig. 7, and cycling behaviors of natural graphite D and the prepared samples N1, N2 and N3 are presented in Fig. 8. As mentioned above, the electrochemical properties of common

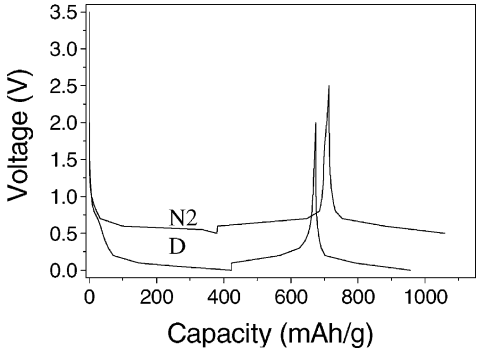

Fig. 7. Discharge and charge profiles in the first cycle and discharge profiles in the second cycle of natural graphite before (D) and after (N2) the mild oxidation with nitric acid solution (for clarity, voltages of N2 were shifted upwards by 0.5 V).

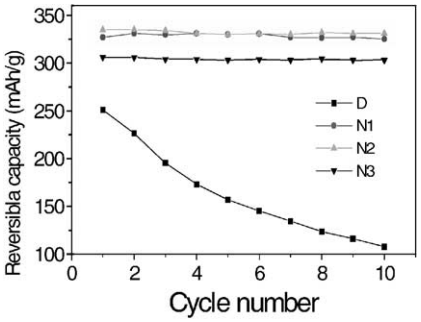

Fig. 8. Cycling behavior of natural graphite before (D) and after (N1, N2 and N3) the mild oxidation with nitric acid solution.

natural graphite without this treatment were poor. Its reversible capacity was only 251 mAh g^{-1}. After the mild oxidation, the reversible capacity of common natural graphite increased to 335 mAh g^{-1}, the irreversible capacity >0.3 V in the first cycle decreased, and the coulombic efficiency in the first cycle increased from 64% to 88%. As observed above, some reactive structural imperfections were eliminated, and therefore, the decomposition of electrolyte molecules was made less likely. In the meantime, the surface of natural graphite was covered with a fresh and dense layer of oxides containing hydroxyl/phenol, ether, ester and carbonyl groups. It acted as a passivating film when lithium intercalated, and blocked the co-intercalation of solvated Li^+. Consequently, the coulombic efficiency increased after the oxidation.

The enhancement of the reversible capacity can be attributed mainly to an increase in the number of micropores through the oxidation treatment. Micropores can act as matrices for lithium storage in the forms of lithium molecules or lithium clusters [1,34,35]. In addition, micropores provide inlets and outlets for lithium during discharge and charge process, and favor lithium intercalation and deintercalation.

The role of the radicals is still not clear from our results. However, since they were situated at the inner of graphite, they did not cause detrimental side reactions. As to their specific actions with lithium, further studies are necessary.

In the case of natural graphite D, the reversible capacity faded to 105 mAh g^{-1} in the first 10 cycles. After the oxidation treatment, its cycling behavior improved much, and there was no evident fading in the reversible capacity independently of the maintained treatment temperatures. Our above results suggest that the stability of natural graphite structure improved and a dense layer of oxides formed after the mild oxidation with the nitric acid solution, therefore, side reactions such as co-intercalation of solvated lithium ions were hindered, and the movement of graphene planes along the *a*-axis became difficult, which resulted in the exploitation or the disruption of graphite [25,27].

Figs. 7 and 8 also suggest that at oxidation temperatures beyond 60 °C, the improvement in the reversible capacity is less pronounced. Most likely the major cause is the rapid decomposition of nitric acid when the temperature was >60 °C. Thus, not all of the chemical oxidant participated in the oxidation reaction and the oxidation effects became less pronounced. However, the electrochemical performance is still good.

4. Conclusion

In summary, the oxidation treatment of natural graphite in the nitric acid solution can also effectively improve its electrochemical performance as anode materials for lithium ion batteries. Through this oxidation, structural imperfections with high reactivity towards lithium such as carbon chains, edge carbon atoms and sp^3-hybridized carbon atoms were eliminated, and more micropores and nanochannels were introduced. In addition, the surface of natural graphite was modified and covered with a dense layer of oxides, which resulted in an increase in the stability of graphite structure, preventing the decomposition of electrolyte constituents and movement of graphene planes along its *a*-axis. Consequently, the reversible capacity enhanced from 251 to 335 mAh g^{-1}, the coulombic efficiency in the first cycle increased from 64% to 88%, and the reversible capacity did not apparently fade though the treatment temperature changed from room temperature to 100 °C.

This kind of oxidation can be used to manufacture anode materials for lithium ion batteries in a large scale. The nitric oxide byproducts formed during the treatment can be recycled by the absorption into nitric acid. The advantage of the liquid–solid interphase oxidation treatment is that the uniformity of the products can be easily controlled. The results also suggest that the requirements for the primary material, natural graphite, are not high and it can be easily available.

Acknowledgements

Financial support from China Postdoctor Foundation and Alexander von Humboldt Foundation is appreciated.

References

[1] Y.P. Wu, C. Wan, C. Jiang, S.B. Fang, Principles, Introduction and Advances of Lithium Secondary Batteries, Tsinghua University Press, Beijing, 2002.
[2] E. Peled, C. Menachem, A. Melman, J. Electrochem. Soc. 143 (1996) L4.
[3] T. Nakajima, K. Yanagida, Tanso 174 (1996) 195.
[4] Y.P. Wu, C.Y. Jiang, C.R. Wan, E. Tsuchida, Electrochem. Commun. 2 (2000) 272.
[5] C. Menachem, Y. Wang, J. Floners, E. Peled, S.G. Greenbaum, J. Power Sources 76 (1998) 180.
[6] T. Takamura, H. Awano, T. Ura, K. Sumiya, J. Power Sources 68 (1997) 114.
[7] H. Buqa, P. Golob, M. Winter, J.O. Besenhard, J. Power Sources 97/98 (2001) 122.

[8] M. Koh, T. Nakjima, Electrochim. Acta 44 (1999) 1713.
[9] M. Yoshio, H.Y. Wang, K. Fukuda, Y. Hara, Y. Adachi, J. Electrochem. Soc. 147 (2000) 1245.
[10] Y. Sato, Y. Kikuchi, T. Nakano, G. Okuno, K. Kobayakawa, T. Kawai, A. Yokoyama, J. Power Sources 81/82 (1999) 182.
[11] R. Mishima, T. Tsuno, S. Yoon, JP Patent, JP 11-329435 (1999).
[12] M. Saito, K. Sumiya, K. Sekine, T. Takamura, Eletrochemistry 67 (1999) 957.
[13] F. Joho, B. Rykart, R. Imhof, P. Nova, M.E. Spahr, A. Monnier, J. Power Sources 81/82 (1999) 243.
[14] S. Yoon, H. Kim, S.M. Oh, J. Power Sources 94 (2001) 68.
[15] Y. Kida, K. Yanagida, A. Funahashi, T. Nohma, I. Yonezu, J. Power Sources 94 (2001) 74.
[16] H. Wang, M. Yoshio, J. Power Sources 93 (2001) 123.
[17] T. Takamura, K. Sumiya, J. Suzuki, C. Yamada, K. Sekine, J. Power Sources 81/82 (1999) 368.
[18] Y.P. Wu, C.Y. Jiang, C.R. Wan, E. Tsuchida, Electrochem. Commun. 2 (2000) 626.
[19] Y.P. Wu, C.Y. Jiang, C.R. Wan, R. Holze, J. Power Sources, in press.
[20] P. Yu, J.A. Ritter, R.E. White, B.N. Popov, J. Electrochem. Soc. 147 (2000) 1280.
[21] H. Huang, E.M. Kelder, J. Schoonman, J. Power Sources 97/98 (2001) 114.
[22] S. Kim, Y. Kadoma, H. Ikuta, Y. Uchimoto, M. Wakihara, Electrochem. Solid-State Lett. 4 (2001) A109.
[23] M. Gaberek, M. Bele, J. Drofenik, R. Dominko, S. Pejovnik, J. Power Sources 97/98 (2001) 67.
[24] M. Saito, K. Sumiya, K. Sekine, T. Takamura, Electrochemistry 67 (1999) 957.
[25] Y.P. Wu, C. Jiang, C. Wan, E. Tsuchida, J. Mater. Chem. 11 (2001) 1233.
[26] Y. Ein-Eli, V.R. Koch, J. Electrochem. Soc. 144 (1997) 2968.
[27] Y.P. Wu, C.Y. Jiang, C.R. Wan, R. Holze, J. Appl. Electrochem., in press.
[28] L.C.F. Blackman, Modern Aspects of Graphite Technology, Academic Press, London, 1970.
[29] G.C. Chung, S.H. Jun, K.Y. Lee, M.H. Kim, J. Electrochem. Soc. 146 (1999) 1664.
[30] J.P. Olivier, M. Winter, J. Power Sources 97/98 (2001) 151.
[31] U. Zielke, K.J. Huttinger, W.P. Hoffman, Carbon 34 (1996) 983.
[32] C. Moreno-Castilla, M.A. Ferro-Garcia, J.P. Joly, I. Bautista-Toledo, F. Carrasco-Marin, J. Rivera-Utrilla, Langmuir 11 (1995) 4386.
[33] Y.P. Wu, C. Wan, C. Jiang, R. Holze, Solid-State Ion., in press.
[34] Y.P. Wu, C. Wan, C. Jiang, S.B. Fang, Y.Y. Jiang, Carbon 37 (1999) 1901.
[35] A. Mabuchi, T. Katsuhisa, H. Fujimoto, T. Kasuh, J. Electrochem. Soc. 142 (1995) 1041.